Design of optical AND, NOR gates using DCF-MZI configuration

LOVKESH[*], NITIKA SHARMA
Department of Electronics & Communication, Punjabi University, Patiala, Punjab, India

In this work, we implement 4-input all-optical NOR and AND logic gate at the data rate of 10 Gbps by exploiting FWM interaction dispersion compensated fiber. In this, we place two dispersion compensated fibers in a Mach-Zehnder interferometric configuration. The system output is investigated in terms of quality factor (Q-Factor), bit error rate (BER) and extinction ratio and finally achieve an extinction ratio of 30 dB.

1. Introduction

Network traffic is increasing rapidly, which increases the high data rate and high bandwidth demand in the network [1-2]. An all-optical network is a promising candidate to fulfil the network demand of high bandwidth [2]. These all-optical systems require ultrafast operations to utilize large optical bandwidth [2-4]. All-optical signal processing elements are the backbone of all-optical system and all-optical logic gates are the basic block to design high speed signal processing elements [1]. These all-optical logic gates can be design by exploiting Kerr's nonlinearities in optical nonlinear medium (semiconductor optical amplifier, highly nonlinear fiber etc.).

To date, various techniques has been proposed by various potential researchers for the design of high-speed all-optical logic gates by the exploitation of four-wave mixing (FWM) [1,4], cross-phase modulation (XPM) [2-3,6], cross-polarization modulation (XPolM) [7] and cross gain modulation (XGM) [8] in semiconductor optical amplifier (SOA) [9-28] and highly nonlinear fiber (HNLF) [1, 3, 29-31]. In [1], Sharma *et al.* exploits the FWM interaction between two co-propagating signals in HNLF to realize all-optical contention detection (AND logic). Singh *et al.* [2] and Lovkesh *et al.* [3], exploits the XPM in highly nonlinear fiber to realize multiple all-optical logic gates. The exploitation of XPM in interferometric configuration is one of the most popular technique to realize the all-optical logic gates [14-16]. However, this configuration requires proper control over the probe signals, as the XPM interaction varies significantly with the variation in probe signal power or operating temperature, which causes the degradation in the extinction ratio (ER) and output quality factor. In addition to this, the exact 180^0 phase shift between the interacting signal is also required to achieve the maximum ER, making the system less flexible and complex. FWM interaction between copropagating signals is another

approach to design all-optical AND gate or wavelength converters [23-25].

From the literature, most of the work is done on the design of only two input optical logic gates. However, the signal processing components requires signal processing operations on multiple optical signals. This requires multiple logic gates for basic operations also. One can reduce the number of logic gates by the design of multiple input all-optical logic gates. So, here we propose a four input all-optical AND and NOR logic gate by the exploitation of FWM interaction in HNLF. The structure of paper is as follows. Section II covers the basic principle behind FWM based optical logic gate design. Section III covers the description of proposed system setup. Section IV covers the brief discussion over the results obtained for proposed design with respect to various operating parameters. And complete finding is covered in section V of the manuscript.

2. Principle of operation

Nonlinear effects in dispersion compensation fibers are performance degrading for optical communication systems. However, these nonlinear effects may be exploited for the realization of all-optical logic gates. When multiple optical signals propagate through nonlinear optical medium (optical fiber, semiconductor optical amplifier), a new frequency signal induces due to the presence of third-order susceptibility in the propagating medium. The frequency of induced signal is the combination of co-propagating signals and are given by equation (1) [1-2, 6].)

$$\omega_{fwm} = \omega_i + \omega_j - \omega_k \; ; i, j, k = 1, 2, 3 \text{ and}, ji, j \neq k \quad (1)$$

Here in equation (1), ω_{fwm} is the induced four-wave mixed-signal frequency and ω_i, ω_j, and ω_k are the

interacting signal frequencies. The total number of induced signals (M) after FWM interaction can be calculated from equation (2) [32].

$$M = \frac{N^2}{2}(N-1) \qquad (2)$$

where N are the total interacting signals co-propagating through the nonlinear medium. The power of the induced signals due to FWM interaction depends on the nonlinear refractive index coefficient, interacting signal power and effective area of the medium which is also given by equation (3) [32].

$$\eta \propto \frac{n_2 p}{A_{eff} D (\Delta\lambda)^2} \qquad (3)$$

Here in equation (3), η is the FWM power conversion efficiency given by the ratio of the power of induced signal and input signal, n_2 is fiber nonlinear refractive index which is a function of the real part of the susceptibility of the medium, P is the interacting signal power, A_{eff} is the fiber effective area and D is the chromatic dispersion coefficient. From equation (3), the FWM induced signal power strictly depends on the power of interacting signals. So, the FWM interaction can be enhanced by using another pump signal in the system which is also exploited in current work. The effective area of fiber plays an important role in FWM interaction and fiber should have low effective area for high efficiency. However, low effective area also causes the enhancement in other Kerr's nonlinearities in the system which may cause the degradation in the systems quality. From equation (3), dispersion should be low for high efficiency. However, the dispersion also causes distortion in the pulse optical signal. This can be eliminated using dispersion compensated fiber (DCF) in the system.

The pictorial representation of FWM interaction when two different frequency signals co-propagate through an optical fiber is also shown in Fig. 1. It shows two input signals at frequency ω_1 and ω_2 co-propagate through an optical fiber. The new signals induced due to FWM interaction inside the optical fiber are also shown at the output port of optical fiber. The frequency of FWM induced signals can be calculated from equation (1).
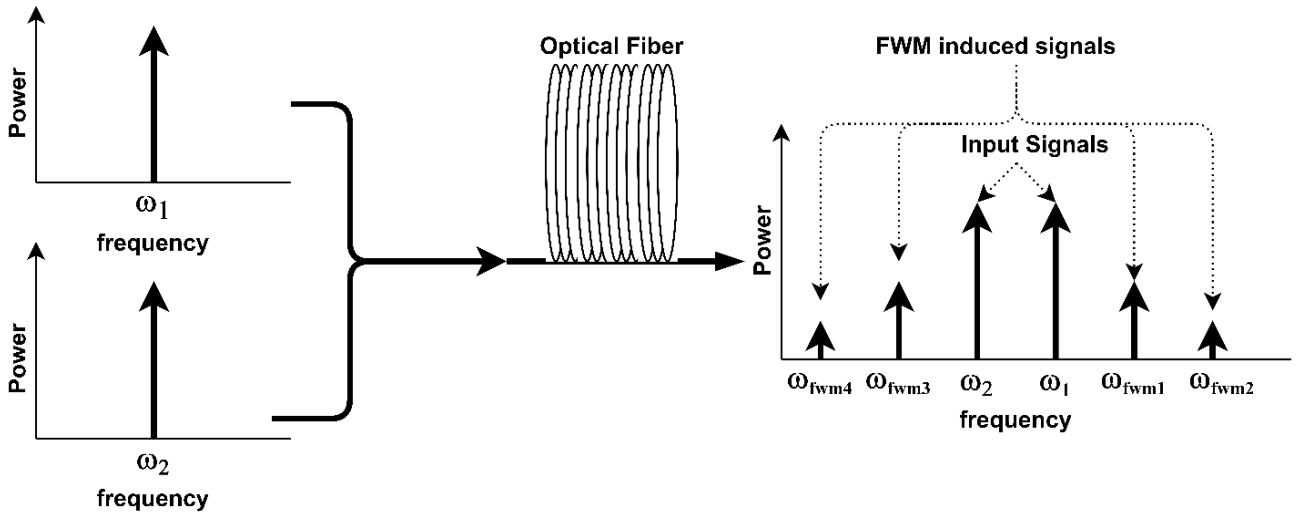

Fig. 1. Optical spectrum representations (a) Before Optical fiber (b) After Optical fiber

The FWM greatly affected by the level of the signal or pump power. The output is rapidly reduced as the pump increases. In addition, it is necessary to have a high relativity pump power to achieve an acceptable logic high at the output. Furthermore, the higher the pump power, better is the quality of the output signal. In addition, if the pump increases too much, all pump pulses will be suppressed, including those that appear as logic high at the output. Four inputs such as A, B, C, and D are used to realize the optical NOR and AND gates. For optical NOR operation, if all the inputs are low then output is high and in the case of AND gate, output is high if all the four channels are high. Truth tables of optical NOR and AND are shown in Table 1 and Table 2. Four signals with different wavelengths λ_1, λ_2, λ_3, λ_4 generated from lasers, boosted with an optical amplifier such as erbium-doped fiber amplifier, and send to multiplexing. A pump is incorporated in the system with four input wavelengths. Two DCFs are placed in MZI configurations for constructive and destructive interference due to phase modulation and new signal generation due to FWM at the output port of MZI. All four wavelengths and a pump passed through DCF-MZI and two ports show different outputs due to constructive and destructive interference. The constructive port is considered to get desired optical logic operation. Two optical filters with different frequencies are required to filter out optical NOR logic and AND logic. For optical NOR operation, if all the inputs are low then output is high and in case of AND gate, output is high if all the four channels are high.

<table>
<tr><td colspan="3">Table 1. Truth Table of optical NOR for 2 inputs</td></tr>
</table>

Table 1. Truth Table of optical NOR for 2 inputs

A	B	Output
0	0	1
0	1	0
1	0	0
1	1	0

Table 2. Truth Table of optical AND for 2 inputs

A	B	Output
0	0	0
0	1	0
1	0	0
1	1	1

3. System setup

Fig. 2 shows the system setup for the realization of 4-input NOR and AND logic at the bit-rate of 10 Gbps. The transmitter provides the 4-inputs at wavelength 1552.52 nm, 1551.72 nm, 1550.92 nm and 1550.12 nm and pump signal at wavelength 1548.52 nm

Fig. 2 shows the system setup with all blocks and components for 4-input NOR and AND logic gate at the date rate of 10 Gbps. The wavelengths of 4 input channels are 1552.52, 1551.72, 1550.92, and 1550.12 nm and the pump wavelength is 1548.52 nm. The CW lasers are incorporated to complete the generation of different laser signals with 10 MHz linewidth. All the laser signals are at 10.87 dBm power with 0.8 nm channel spacing. Binary data is generated from a user-defined pseudo-random bit generator followed by non-return to zero modulation format, which maps the pseudo-random bit generator output with an electrical binary signal which modulates the optical signal propagating through the electro-optic intensity modulator.
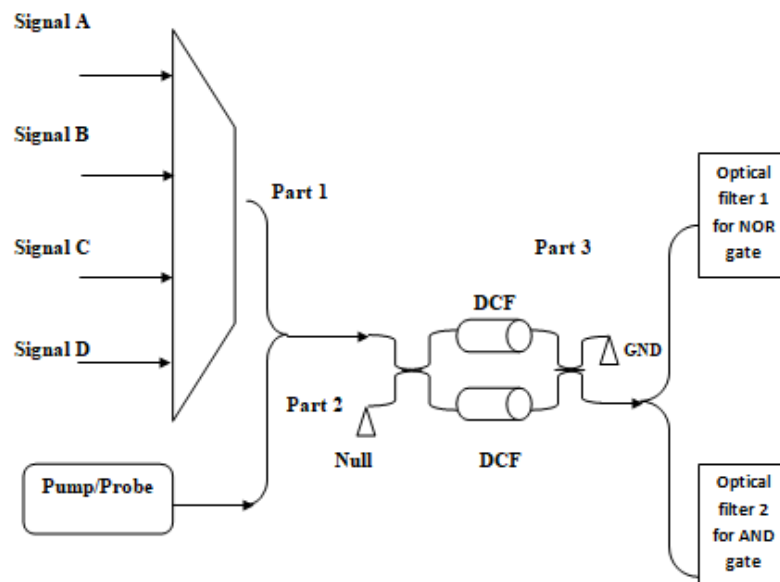

Fig. 2. Block diagram of 4 input DCF-MZI based optical NOR and AND logic

Table 3. Parameters of the proposed system

Parameters	Values
Total input wavelengths	4
Wavelengths of input signals	1552.52, 1551.72, 1550.92, and 1550.12 nm
Modulator used	MZM with 20 dB extinction ratio
Optical amplifier	EDFA
Total EDFAs	2
Gain of EDFA1 and EDFA 2	15 and 25 dB respectively
Nonlinear medium	DCF
Total DCF used	2
Configuration	MZI-DCF
DCF length (each)	0.07 Km
Effective area of DCF and attenuation	10 μm^2 and 0.5 dB/Km respectively
Optical filter frequencies	1548.52 nm (NOR), 1546.96 nm(AND)

All four transmitters consist of these components. Signals are combined by using power combiner and erbium-doped fiber amplifier having 15 dB gain and 5 dB noise figure. Further, another multiplexer is incorporated in the system to accumulate the transmitter section and receiver section of the proposed system and shown in Figs. 3(a) and 3(b), respectively for amplified signals. The power of the pump signal is -9.6 dB and linewidth is 10 MHz. Multiplexed four input signals and one pump signal are then fed to DCF-MZI module after amplifying through EDFA2 of 25 dB gain. In this module, two DCF fibers are placed in the upper and lower arm of the MZI interferometer. The length of each fiber is 0.07 km and the effective area is 10 μm^2. Parameters of the proposed system are given in Table 3.
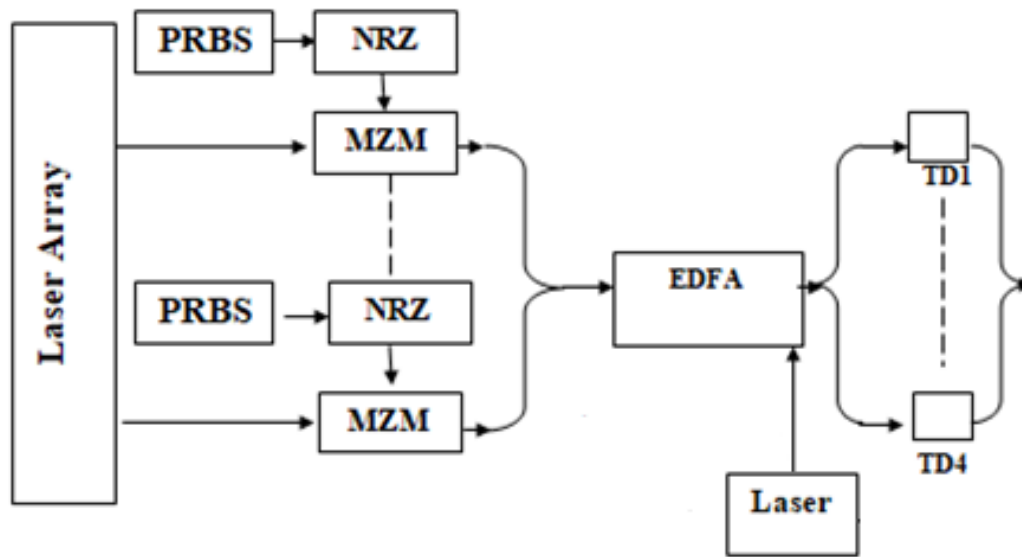

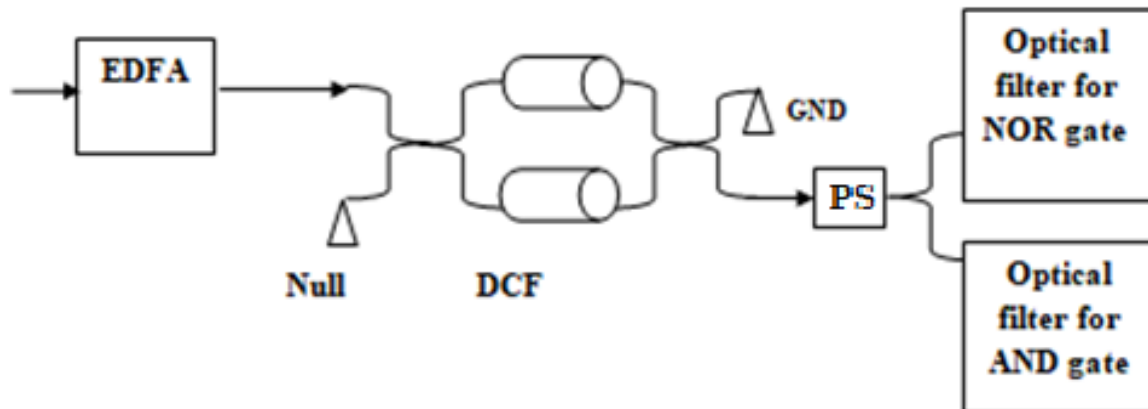*Fig. 3(a). Block diagram of 4 port optical transmitter design*

Fig. 3(b). Representation of DCF-MZI (channel) and receiver of proposed system

Further, the signal from the lower port of X-coupler is followed by a power splitter. The signal from the upper port and lower port of the power splitter are followed by 0.8 bandwidth bandpass filters at wavelength 1548.52 nm and 1546.96 nm respectively. The bandpass filter of having 148.52 nm central wavelength gives the NOR logic and filter having wavelength 1546.96 nm gives the AND logic. Further the signal from bandpass filter are followed by electrical receivers which consists of phot-diodes followed by electrical low pass filter, 3-R regenerator and eye diagram analyzer.

4. Results and discussions

Investigation of proposed all-optical NOR and AND gate has been done at low signal powers by using simple architecture discussed in previous section. Four input signals at wavelength 1550.12 nm, 1550.92 nm, 1551.72

nm and 1552.52 nm and pump signal at wavelength 1548.52 nm. The wavelength of the input signal and pump signal are chosen in such a way that no inter-channel interference will occur in the system. The system setup for the generation of input message signal consists of electrical signal generator, laser source and a Mach-Zehnder modulator, which is also briefly discussed in previous section. Further, all the input signal sources give the input to the 4×1 multiplexer. Further the input signal gets combined with pump signal using power combiner. The spectrum diagram of optical signal at the output port of power combiner is given by Fig. 4.
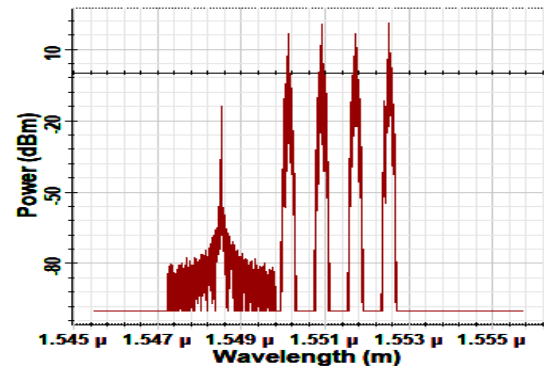

Fig. 4. Optical spectrum analyzer of four signals and one pump signal
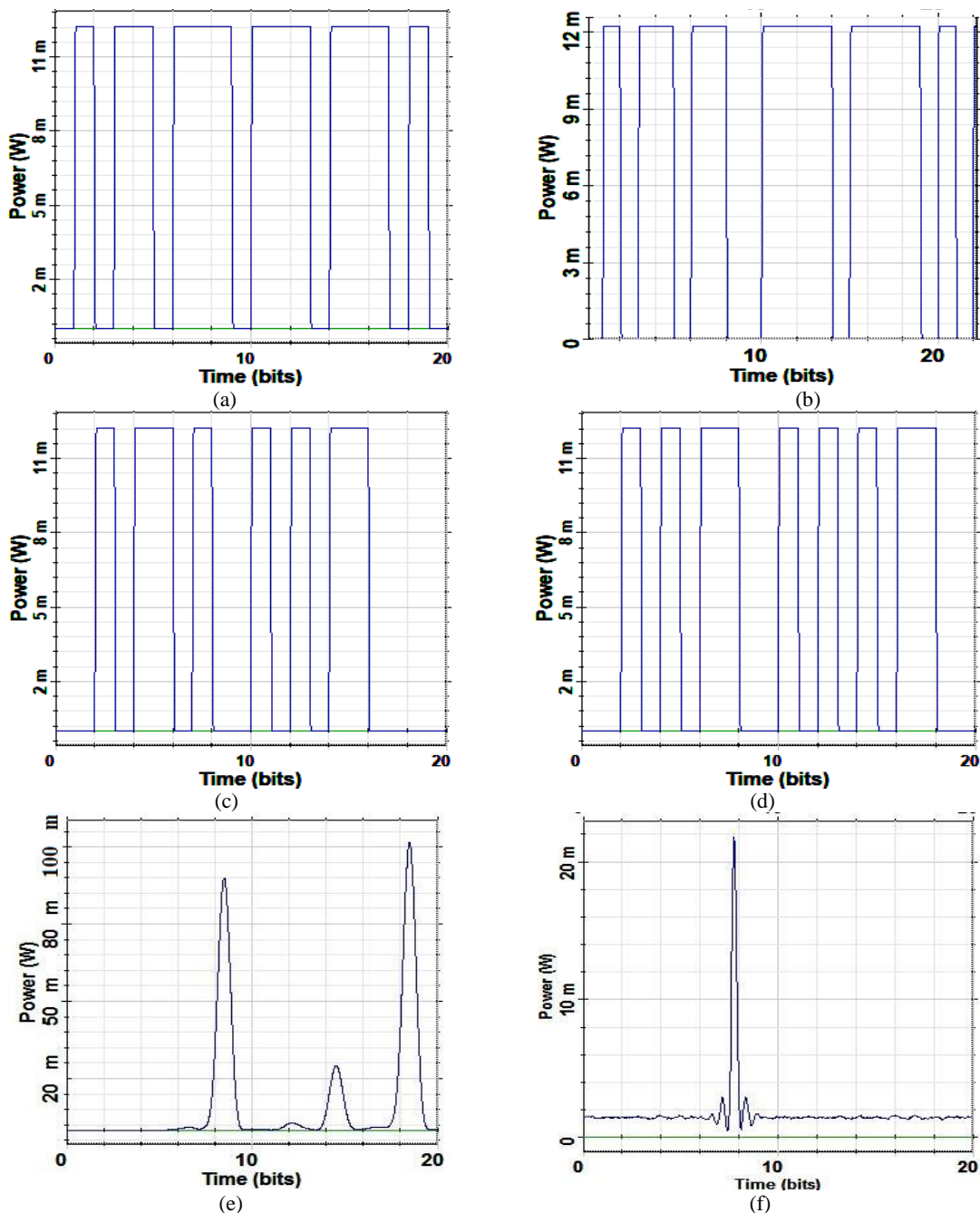

(a)

(b)

(c)

(d)

(e)

(f)

Fig. 5. Optical time domain analyzer for (a) data Input 1 (b) data Input 2 (c) data Input 3 (d) data Input 4, (e) output NOR logic and (f) output AND logic (color online)

Optical time domain visualizer is an analyzer incorporated after each modulated wavelength channel to represent the bits with their time slots and amplitude. Data rate is 10 Gbps and therefore bit slot is 0.1 ns. Fig. 5(a), (b), (c) and (d) depicts the output of optical time domain visualize. Total 20 bits in one sequence are considered.

Further the combined signal from power combiner is followed by a DCF-MZI switch. FWM interaction occur inside the fiber. To enhance the FWM interaction, power is boosted with erbium doped fiber amplifier (EDFA) having 25 dB gain and 4 dB noise figure. FWM occurred in DCF-MZI and signal passed through upper and lower port of MZI switch. The MZI switch consists of X-coupler at the output port and optical signals shows destructive interference at the upper output port and constructive interference at lower output port. The spectrum diagram of optical signals at the lower port, filtered signal for NOR gate operation and filtered signal for AND gate operation are shown in Fig. 6(a)-(c) respectively.
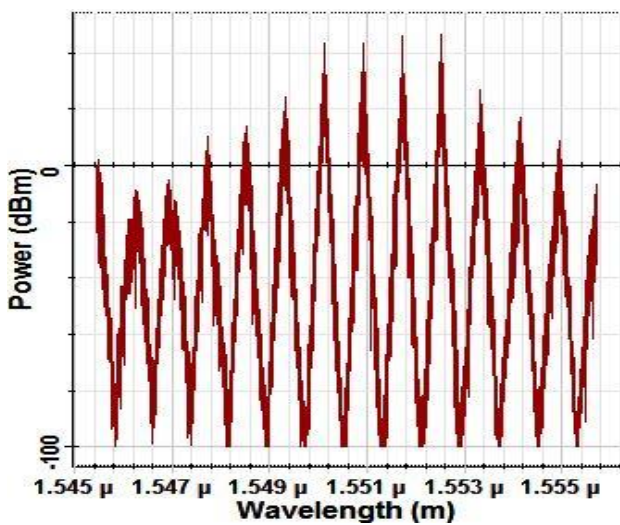
(a)
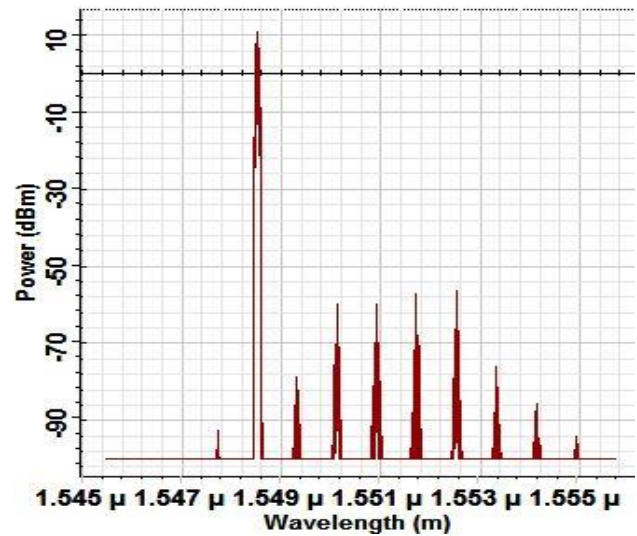
(b)
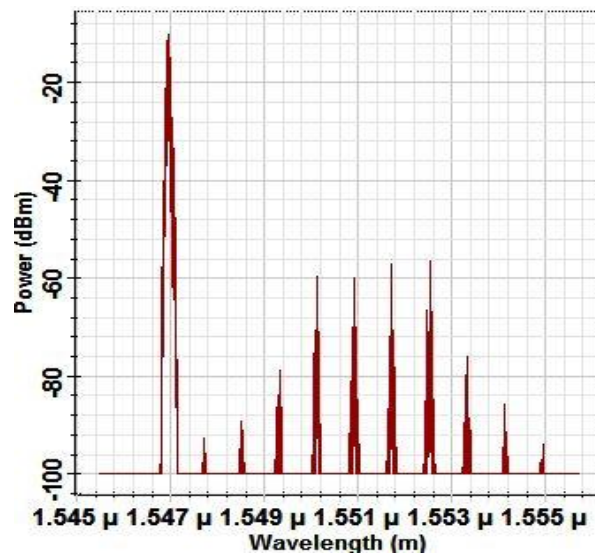
(c)

Fig. 6. Optical spectrum at the (a) lower port of DCF-MZI (b) filtered wavelength of NOR gate (c) filtered wavelength of AND gate

The signal from constructive port is followed by a power splitter and then followed by optical amplifiers to enhance the systems sensitivity. Further the signal is filtered out by using 0.8 nm bandwidth band pass filter at wavelength 1548.52 nm to realize an all-optical NOR gate operation. The spectrum for NOR gate operation is also show in Fig. 6(b). The other port of the power splitter is also followed by a signal enhancer optical amplifier followed by a 0.8 nm bandwidth band-pass filter at wavelength 1546.96 nm for the realization of all-optical AND gate operation. The spectrum diagram for all-optical AND gate operation is also shown in Fig. 6(c). It is observed that filter suppressed other wavelengths and allow passing intended signal only. It is discussed that an optical filter with wavelength of 1548.52 nm is deployed for NOR gate and filter is having bandwidth of 0.8 nm. Therefore, an optical time-domain analyzer is placed after optical filter such that it can represent the optical bits received after filters.

Fig. 6(b) shows the output of optical time domain analyzer for optical NOR gate. It is perceived that received power of 110 mW has been observed at the receiving end. Table of inputs and outputs for transmitted binary data is shown in Table 4.

Table 4. Input and output bits of optical NOR gate

A	B	C	D	Output
0	1	0	0	0
0	0	1	1	0
1	1	0	0	0
1	1	1	1	0
0	0	1	0	0
1	1	0	1	0
1	1	1	1	0
1	0	0	0	0
0	0	0	0	1
1	1	1	1	0
1	1	0	0	0
1	1	1	1	0
0	1	0	0	0
1	0	1	1	0
0	1	1	0	0
1	1	0	1	0
1	1	0	1	0
1	1	0	0	0
0	0	0	0	1

Wavelength 1546.96 nm is employed to for the filter's optical AND gate and bandwidth is 0.8 nm. An optical time-domain analyzer is placed after optical filter to represent the optical bits received after filters for optical AND gate. Fig. 6(f) shows the output of optical time domain analyzer for optical AND gate. Results revealed that received power of 20 mW has been observed. Table of

inputs and outputs for transmitted binary data for optical AND gate is shown in Table 5.

Table 5. Input and output bits of optical AND gate

A	B	C	D	Output
1	1	0	0	0
0	0	1	1	0
1	1	0	0	0
1	1	1	1	0
0	0	1	0	0
1	1	0	1	0
1	1	1	1	1
1	0	0	0	0
0	0	0	0	0
1	1	1	1	0
1	1	0	0	0
1	1	1	1	0
0	1	0	0	0
1	0	1	1	0
0	1	1	0	0
1	1	0	1	0
1	1	0	1	0
1	1	0	0	0
0	0	0	0	0

Further the effect of launched power in DCF-MZI system on the quality factor (Q-factor) of the all-optical NOR and AND logic operation is plotted in Fig. 7(a). The Q factor can be calculated from equation (4).

$$Q = \frac{I_1 - I_0}{\sigma_0 + \sigma_1} \qquad (4)$$

Here in equation (4), I_1 and I_0 are the power level for logic high and logic low respectively and σ_0 and σ_1 are standard deviation for logic low and logic high respectively.

To study the effect of power, the launched power is varied from -5 dB to 20 dB with the difference of 5 dB. From the plot, it is observed that, initially, with an increase in launched power, the Q-factor also increases linearly and for bot AND and NOR logic. The Q-factor reaches to the peak point of 10.56 dB for AND logic and 7.9 dB for NOR logic for 10 dB launched power. The quality factor increases due to the increase in the FWM interaction due to an increase in interaction signal power. From the plot, further increase in launched power, the slope of Q-factor become negative. Number of factors also may degrade the quality of received signal. The XPM and SPM and Raman scattering also increases with an increase in launched signal power which causes the degradation in the signal quality. These nonlinear effects overcome the effect of FWM interaction and causes the degradation in the Q-factor of the signal.
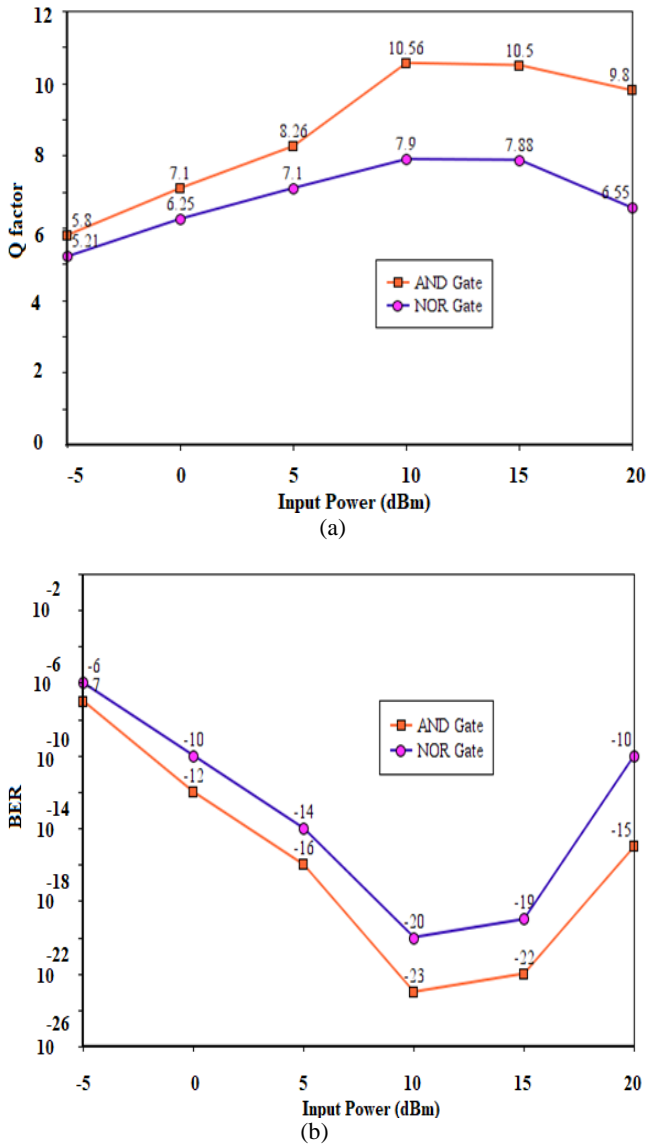
Fig. 7. Variation of (a) Q factor (b) BER with input power
for optical NOR and AND gate (color online)

Again, power of the signals is varied from -5 dB to 20 dB with the difference of 5 dB to obtain the effect of launched power on BER. BER is a function of Q-factor and can be calculated from equation (5).

$$BER = \frac{1}{2}erfc(\frac{Q}{\sqrt{2}}) \qquad (5)$$

where Q is quality factor, *erfc* is the error function and is a special function of sigmoid shape that occurs in probability, statistics, and partial differential equations describing diffusion.

Further the effect of input signal power on output BER for all-optical NOR and AND logic is plotted in Fig. 7(b). For a better system, the BER should be low. From the plot, initially for -5 dB input power, BER is very high and not suitable for an optical system. With an increase in signal power, the BER starts decreasing. The BER starts decreasing due to an increase in the FWM interaction with an increase in interacting signal power. The BER level

reaches to the minimum point for 10 dB input signal power. With an increase in interacting power, the other nonlinear effect also come into the picture causes the increase in the BER with further increase in input signal power. From the plot shown in Fig. 7(a) and (b), the input power should be high for high output quality. But not too high, so that other nonlinearities degrade the quality of the system.

The eye diagram is an intuitive graphical representation of electrical and optical communication signals. The quality of these signals (the amount of inter-symbol interference (ISI, noise, and jitter) can be judged from the appearance of the eye. Eye diagram of the optical AND and NOR gates provide information about Q factor, BER, threshold, eye opening, eye closer, jitter, etc. These are essential parameters to evaluate the system performance. Eye diagram represents the average level of 1's and 0's in fixed time slot. More is the average amplitude of 1's, more is the opening of eye, and in turn more is the Q factor. Eye diagram for NOR gate is shown in Fig. 8 (a).
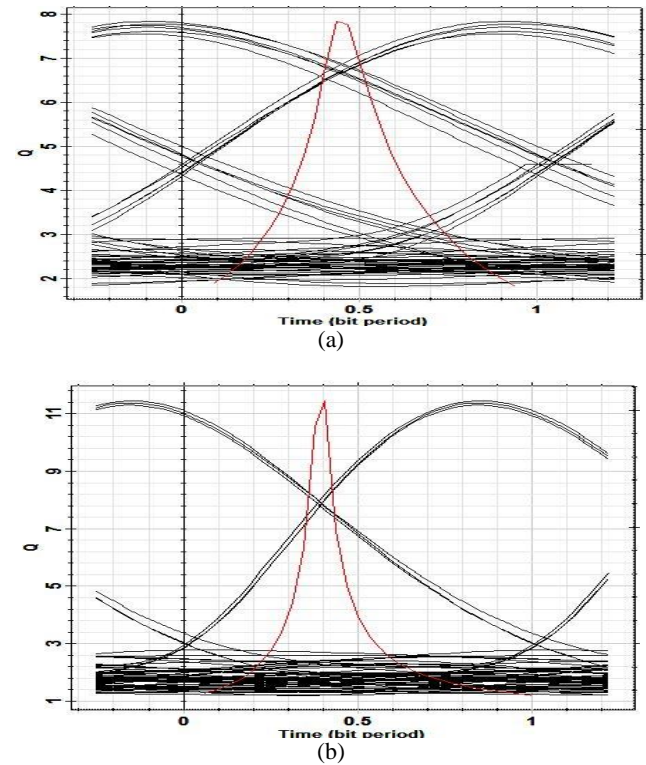

Fig. 8. Eye diagram of (a) optical NOR gate (b) optical
AND gate at 10 Gbps (color online)

Further, in Fig. 8(b), the eye diagram of optical AND gate is depicted at 10 Gbps and it is perceived that opening of eye is more in optical AND gate than optical NOR gate. Value of jitter is less in optical AND gate and therefore eye opening is more. The eye diagram is an intuitive graphical representation of electrical and optical communication signals. The quality of these signals (the amount of inter-symbol interference (ISI, noise, and jitter) can be judged from the appearance of the eye.

5. Conclusion

The results obtained in this paper led us to conclude that, a four input all-optical NOR and AND gate can design by the exploitation of FWM interaction in a highly nonlinear fiber. To maximize the FWM interaction in optical fiber, fiber should have low effective area and high nonlinear refractive index. The FWM interaction also increases with an increase in interacting signal powers. The increase in FWM interaction also causes the increase in the quality and decrease in the bit error rate of output signal. However, the increase in interacting signal power also causes the increase in other nonlinear effects which may degrades the quality of the system. So the power level should be optimized to achieve better quality at the output power. For better optical logic gates, quality factor should be high and bit error rate should be low. The proposed logic gates have the capability to perform various optical signal processing operations to cope with the demand of future high-speed optical networks. In future, we plan to extend the proposed optical logic gates to design the various all-optical components like, adder, multiplier, subtractor, parity checker, shift registers, contention detectors which can be easily contracted.

Acknowledgment

References

[1] Surinder Singh, Dilbag Singh, Vishal Sharma, Sukhbir Singh, Quang Minh Ngo, Optical Fiber Technology **52**, 202958 (2019).

[2] Dilbag Singh, Surinder Singh, Vishal Sharma, Sukhbir Singh, Quang Minh Ngo, Optical and Quantum Electronics **51**, 215 (2019).

[3] Lovkesh, Vishal Sharma, Surinder Singh, Journal of Computational Electronics **20**, 397 (2021).

[4] B. Vasavi, C. Bhargava, K. H. Chowdary, Int. J. Inf. Commun. Technol Res. **2**(2), 112 (2012).

[5] A. Bogoni, X. Wu, I. Fazal, A. E. Willner, J. Lightwave Technol. **27**(19), 4221 (2009).

[6] K. Singh, Kaur, Proceedings of International Conference on Recent Innovations in Engineering and Technology, Abu Dhobi, 40–46, (2014).

[7] J. Qiu, K. Sun, M. Rochette, L. R. Chen, IEEE Photon. Technol. Lett. **22**(16), 1041 (2010).

[8] Wnrui Wang, Jinlong Yu, Bingehn Han Jingzhong Guo, Jun Luo, Ju Luo, Optoelectronic Materials and Devices VI, edited by Guang-Hua Duan, Proc. of SPIE-OSA-IEEE Asia Communications and Photonics, SPIE **8308**(086) 1 (2011).

[9] D. N. S. Cavalcante, J. S. Negreiros, Jr., L. R. Marcelino, J. I. S. Miranda, R. R. Barboza, L. S. P. Maia, G. M. Medeiros, G. F. Guimarães, IEEE Photonics Technology Letters **31**(1), 1 (2019).

[10] Dimitrios E. Fouskidis, Kyriakos E. Zoiros, Antonios Hatziefremidis, IEEE Journal of Selected Topics in Quantum Electronics **27**(2), 7600915, (2021).

[11] Surinder Singh, Lovkesh, Xiaohua Ye, R.S. Kaler, IEEE Journal of Quantum Electronics **48**(12), 1547 (2012).

[12] Y. Aikawa, S. Shimizu, H. Uenohara, Journal of Lightwave Technology **29**(15), 2259 (2011).

[13] G. Berrettini, A. T. Nguyen, E. Lazzeri, G. Meloni, M. Scaffardi, L. Potı, A. Bogoni, IEEE Journal of Selected Topics in Quantum Electronics **18**(2), 847 (2012).

[14] Amer Kotb, Kyriakos E. Zoiros, Chunlei Guo, Optics and Laser Technology **108**, 426 (2018).

[15] Amged Alquliah, Amer Kotb, Subhash C. Singh, Chunlei Guo, Optik - International Journal for Light and Electron Optics **225**, 165901 (2021).

[16] Surinder Singh, Lovkesh, IEEE Journal of Selected Topics in Quantum Electronics **18**(2), 970 (2012).

[17] Kousik Mukherjee, Optics & Laser Technology **140**, 107043 (2021).

[18] Amer Kotba, Kyriakos E. Zoiros, Chunlei Guo, Optics and Laser Technology **119**, 105611 (2019).

[19] Dimitrios E. Fouskidis, Kyriakos E. Zoiros, Antonios Hatziefremidis, IEEE Journal of Selected Topics in Quantum Electronics **27**(2), 7600915, (2021).

[20] Nivedita Nair, Sanmukh Kaur, Hardeep Singh, Optik - International Journal for Light and Electron Optics **231**, 166325 (2021).

[21] Yaya Mao, Bo Liu, Rahat Ullah, Tingting Sun, Lilong Zhao, Optics Communications **466**, 125421 (2020).

[22] Lovkesh, Sandeep Singh Gill, Optik **122**(11), 978 (2011).

[23] Xin Chen, Li Huo, Zhixi Zhao, Liang Zhuang, Caiyun Lou, IEEE Photonics Technology Letters **28**(21), 2463 (2016).

[24] Amer Kotb, Chunlei Guo, Optics & Laser Technology **137**, 06828 (2021).

[25] Evangelia Dimitriadou, Kyriakos E. Zoiros, Journal of Lightwave Technology **31**(23), 3813 (2013).

[26] Lovkesh, Anupma Marwaha, Optics & Laser Technology **70**, 112 (2015).

[27] Shu-Chao Mi, Hai-Long Wang, Shu-Yu Zhang, Qian Gong, Optik - International Journal for Light and Electron. Optics **202**, 163551 (2020).

[28] Ammar Sharaiha, Joseph Topomondzo, Pascal Morel, Optics Communications **265**, 322 (2006).

[29] Jian Wang, Qizhen Sun, Junqiang Sun, Xinliang Zhang, Optics Communications **282**(13), 2615 (2009).

[30] Lanlan Li, Jian Wu, Jifang Qiu, Bingbing Wu, Kun Xu, Xiaobin Hong, Yan Li, Jintong Lin, Optics Communications **283**(19), 3608 (2010).

[31] P. Velanas, A. Bogris, D. Syvridis, Optical Fiber Technology **15**(1), 65 (2009).

[32] Emam S. Azzam, Moustafa H. Aly, Optical and Quantum Electronics **50**, 166 (2018).

_____

[*]Corresponding author: lovkesh_bhatia@yahoo.in